



Article

The Effect of Droughts on Vegetation Condition in Germany: An Analysis Based on Two Decades of Satellite Earth Observation Time Series and Crop Yield Statistics

Sophie Reinermann ^{1,*} , Ursula Gessner ², Sarah Asam ² , Claudia Kuenzer ^{1,2} and Stefan Dech ^{1,2}

¹ Department of Remote Sensing, Institute of Geography and Geology, University of Wuerzburg, 97074 Wuerzburg, Germany

² German Remote Sensing Data Center (DFD), Earth Observation Center (EOC), German Aerospace Center (DLR), 82234 Wessling, Germany

* Correspondence: sophie.reinermann@dlr.de

Received: 19 June 2019; Accepted: 25 July 2019; Published: 30 July 2019



Abstract: Central Europe experienced several droughts in the recent past, such as in the year 2018, which was characterized by extremely low rainfall rates and high temperatures, resulting in substantial agricultural yield losses. Time series of satellite earth observation data enable the characterization of past drought events over large temporal and spatial scales. Within this study, Moderate Resolution Spectroradiometer (MODIS) Enhanced Vegetation Index (EVI) (MOD13Q1) 250 m time series were investigated for the vegetation periods of 2000 to 2018. The spatial and temporal development of vegetation in 2018 was compared to other dry and hot years in Europe, like the drought year 2003. Temporal and spatial inter- and intra-annual patterns of EVI anomalies were analyzed for all of Germany and for its cropland, forest, and grassland areas individually. While vegetation development in spring 2018 was above average, the summer months of 2018 showed negative anomalies in a similar magnitude as in 2003, which was particularly apparent within grassland and cropland areas in Germany. In contrast, the year 2003 showed negative anomalies during the entire growing season. The spatial pattern of vegetation status in 2018 showed high regional variation, with north-eastern Germany mainly affected in June, north-western parts in July, and western Germany in August. The temporal pattern of satellite-derived EVI deviances within the study period 2000–2018 were in good agreement with crop yield statistics for Germany. The study shows that the EVI deviation of the summer months of 2018 were among the most extreme in the study period compared to other years. The spatial pattern and temporal development of vegetation condition between the drought years differ.

Keywords: drought; time series; heat wave; agriculture; climate extremes; climate change; crop statistics; MODIS; Germany

1. Introduction

The 2018 growing season was extremely warm and dry in central Europe, and the months April to August were amongst the most extreme in the recent past regarding meteorological parameters [1]. It is expected that such extreme summers will occur more frequently in future. According to the latest reports of the Intergovernmental Panel on Climate Change (IPCC), surface temperatures will rise over the 21st century. It is very likely that heat waves will be more intense, more frequent, and last longer, and that risk levels regarding water restrictions and damages from extreme temperatures for Europe

will increase [2,3]. With 2 °C of global warming, one out of every two summer months in Europe could show higher temperatures than ever observed under current climate conditions [4]. Several recent studies show that, by the end of this century, drought events will become more frequent all over Europe [5–7].

The projected increase of climate extremes is likely to have severe consequences on environmental, economic, and infrastructure systems as well as on human health in Europe. In the aftermath of the summer of 2003 heat wave, the deaths of thousands of vulnerable elderly people in Europe were reported [8]. Different ecological systems show varying degrees of resilience to an increase in droughts. Long-term consequences are possible shifts in species composition, ecosystem degradation, and loss of ecosystem services [9]. For example, ecosystems such as forests and bogs will be affected by an increased risk of wildfires. Furthermore, the carbon sequestration potential is strongly reduced under drought conditions, with a projected overall decrease in vegetation carbon uptake over Europe [10], further reinforcing the drivers of climate change. The agricultural sector is harmed as crop yields [11] and above-ground biomass of grasslands [12] will be reduced. An increased information need on crop failure estimates will arise for farmers, insurance providers, and public authorities alike.

While the drought situation in 2018 was not uniform for all of Europe, with some southern regions registering below-average temperatures and high precipitation [1,13], the spring and summer of 2018 in Germany, like in other central and north European countries, were characterized by extraordinarily dry and warm conditions [13,14]. The average temperatures in June–August were the second hottest since the beginning of recordings in 1881 and were only exceeded by temperatures in 2003 [13]. A strong rainfall deficit was registered for the north and central-east of Germany, where summer precipitation sums were lowest or second lowest since 1881, while the negative anomalies were not as strong for southern and north-eastern regions [13]. This meteorological drought resulted in an agricultural drought in large parts of Germany. In reaction to the adverse effect of drought and heat conditions on the agricultural sector in 2018 in Germany, federal aid payments of 340 million Euros were warranted to farmers with at least 30 percent of yield loss [15].

However, so far, the characteristics of the agricultural drought in Germany in 2018 have not yet been analyzed based on earth observation data, and its patterns have not yet been compared to other drought years. Within this study, we assess the condition of the vegetation in 2018, compare it to other years within the last two decades, and reveal interesting patterns using satellite earth observation data. In previous studies, drought and heat conditions in Europe were analyzed using climatological, vegetation and hydrological data partly based on satellite earth observation, which enables extensive investigations over varying land cover and ecosystem types. In particular, with regard to agricultural droughts, the examination of satellite-based vegetation indices has become an important method as no field measurements, interpolation, or large-scale modelling are required. For investigating vegetation status under extreme conditions, several medium-resolution satellite data sets (e.g., AVHRR, Spot-VEGETATION, MERIS, MODIS, and SeaWiFS) were used in previous studies [16–24]. When investigating the influence of climate extremes on agriculture, the focus lies on the assessment of the reaction of plants toward extreme climate conditions. The reaction of plants is majorly linked to ecosystem services, such as carbon sequestration, and economic factors, such as yield loss. In previous studies, extreme conditions of plant properties were already investigated using satellite-based proxies of vegetation vitality and/or productivity. The most prominent investigated parameters in this regard are vegetation indices, such as NDVI [16–18,21,23], and modelled productivity estimates, such as fraction of absorbed photosynthetically active radiation (FAPAR) [19,25], net primary productivity (NPP) [10], and gross primary productivity (GPP) [20,22,26]. Previous studies analyzing the reaction of plants toward climate extremes found temperate regions to show rapid responses of vegetation vitality and productivity [21,23]. In addition, it was revealed in a previous study that terrestrial ecosystems in the mid latitudes exhibit a poor resilience toward droughts with more than 60 days of recovery time [20]. To our best knowledge, none of the presented indices and parameters was identified as being optimal for all land cover and ecosystem types, and they are often consistent

among each other. Additionally, most of these studies used meteorological parameters as indicators for drought, like Standardized Precipitation Index (SPI) [17,18,23], Standardized Precipitation Evaporation Index (SPEI) [21], or soil moisture [22,27], and investigated the reaction of the vegetation during their previously detected climate extremes. However, extreme vegetation reactions and climate extremes often have a non-linear relationship, as extreme reactions within the vegetation are possibly induced by an accumulation or specific combination of climatic conditions that would not be extreme when considered separately [28,29]. Therefore, within this study, we base the investigation on the vegetation reaction (impact-based) [19] and focus solely on the dynamics of vegetation condition in Germany within the last 19 years.

In order to investigate vegetation stress in Germany within the past two decades, we use a robust and straightforward approach to detect temporal and spatial patterns of vegetation condition derived by earth observation data. Within this study, Moderate-resolution Imaging Spectroradiometer (MODIS) Enhanced Vegetation Index (EVI) time series of the meteorological vegetation period (March to November) from 2000 to 2018 were investigated. The aim of the study was to reveal the drought characteristics (strength, variability, and patterns) in Germany in 2018, to identify potential regional differences, and compare the situation to other dry and hot years, like the drought year 2003. To examine the drought effects in various land cover types, the analysis was also conducted for cropland, grassland, and forest areas individually. In addition, annual crop statistics are analyzed to assess the impact of agricultural drought on crop production.

2. Study Region

The study focuses on Germany, with a total area of 357,168 km² (Figure 1). Germany's elevation ranges from 2962 m above sea level in the Alps to sea-level at the North and Baltic Seas. The country is located in the west wind zone and is characterized by a temperate seasonal climate, ranging from temperate sub-oceanic to temperate sub-continental climate. The typical average values of temperature (Jan: −0.5 °C/Jul: 17.1 °C) and precipitation (Feb: 40 mm/Jun: 77 mm) show strong regional differences and can be, in case of extreme weather situations, considerably higher or lower [30]. Germany comprises approximately 33% arable land, 13% pastures, 31% forest and woodland, 2% water bodies, 14% covered by human structures, and the remaining 7% listed as other [31]. The largest proportion of arable land consists of wheat with 26%, which mainly consists of winter wheat [31]. Rye and winter cereal constitute 5%, potatoes 6%, and silage maize 19% of the arable land in Germany [31].

The regional statistical analyses in this study have been conducted on the national scale (NUTS-0) and on the administrative entities of counties ("Landkreise", NUTS-3).

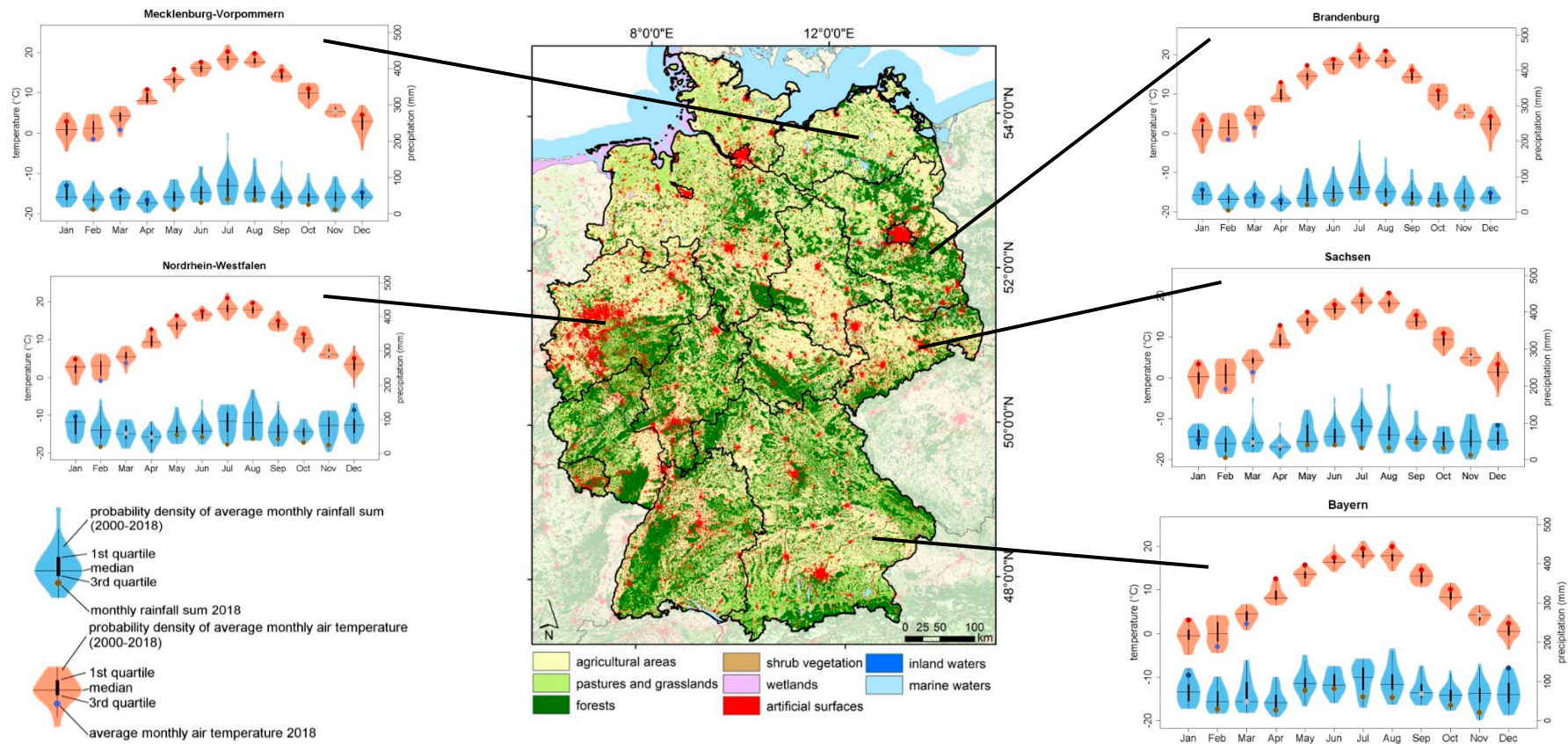


Figure 1. Land use/cover types of Germany (central panel) and annual distribution of temperature and precipitation for selected German federal states (right and left panel). Data source: land use/cover data: CORINE land cover 2012 [32]; climate data: [30].

3. Materials and Methods

3.1. Input Data

The presented analyses are based on the complete 250 m resolution Terra MODIS Enhanced Vegetation Index (EVI) time series covering the years 2000 until 2018. Vegetation indices (VI) are established tools to highlight vegetation vigor and productivity while reducing the effects of acquisition geometry, atmospheric conditions, and soil properties on the remotely sensed signal. Since our own pre-analyses indicated a higher robustness of the EVI in comparison to other VIs such as NDVI, this metric was chosen for further analysis. The EVI has a value range from -1 to 1 , with values below 0 generally corresponding to non-vegetated areas. The EVI is, like other VIs, a proxy for the vitality and productivity of the vegetation. However, it is also influenced by the structure, density and phenological stage of the vegetation, which is why we do not use absolute but relative EVI values to investigate the vegetation condition in this study. Sixteen-day composites of EVI and the corresponding pixel reliability layers were extracted from the MODIS product MOD13Q1, version 6 [33]. All available 16-day composites per year were included in the multi-annual MODIS time series, starting with the composite of 18 February 2000 and ending with the composite of 19 December 2018. The composite dates represent the starting dates of the 16-day MODIS EVI composites.

In order to assess the effect of agricultural drought conditions on crop production in Germany, crop yield statistics from the federal statistics agency of Germany (Destatis) were used. The annual yields per hectare for Germany for four different crop types (winter wheat, rye and winter cereal, silage maize, and potatoes) were examined [31]. The CORINE land cover (CLC) map of 2012 Version 18.5.1 and the CORINE land cover change (LCC) layers (2000–2006 and 2006–2012) Version 18.5 [32], all with a spatial resolution of 100 m, were used for masking and for land cover specific analyses.

3.2. Data Processing and Analysis

The analysis of drought and heat effects on vegetation in Germany was based on the assessment of deviations of MODIS 16-day EVI measurements from their long-term (19-year, 2000–2018) averages.

Data processing was conducted on the Google Earth Engine platform (<https://earthengine.google.com/>) [34], from which the MODIS data was also provided. The MODIS dataset was mosaicked and resampled from sinusoidal to the WGS 84 reference coordinate system by the nearest neighbor method during processing. To avoid the analysis of MODIS observations of low quality, the MODIS “pixel reliability” layer was considered, and all pixels that did not show best quality (class 0) were excluded from further processing. In order to restrict the analysis of drought and heat effects to vegetated areas, all EVI values below zero were excluded from further processing, and additionally all areas were masked where the CORINE land cover/use dataset of the year 2012 indicated non-vegetated land cover classes “urban” and “water.” Further—to avoid confusions of drought impacts with land cover/use change related effects—all areas that showed land use/cover changes in the CLC change products for 2000–2006 and 2006–2012 were masked.

For each 16-day composite, the 18-year median EVI was calculated based on the MODIS time series (see Figure 2). Subsequently, the deviation of each individual composite of the multi-annual time series from the respective long-term composite median of the same 16-days period was calculated. These 16-day deviations were then averaged to monthly and seasonal (i.e., spring: March–May; summer: June–August; autumn: September–November) intervals in order to minimize outlier effects. Each monthly anomaly was built with the two 16-day anomalies, for which most days lay within the month of interest. This led to one 16-day anomaly being included in two monthly means (April and May), as the 16-day composite of the 23rd of April consists of eight days in April and eight days in May (see Table 1). The MODIS data shows data gaps during winter due to higher cloud coverage and poorer lighting conditions and the deviations are probably highly affected by snow cover. Therefore, only the spring to autumn periods (March–November) of every year were used in this study. The pixel-based seasonal and monthly deviations were aggregated to counties (“Landkreise”, NUTS-3) by averaging.

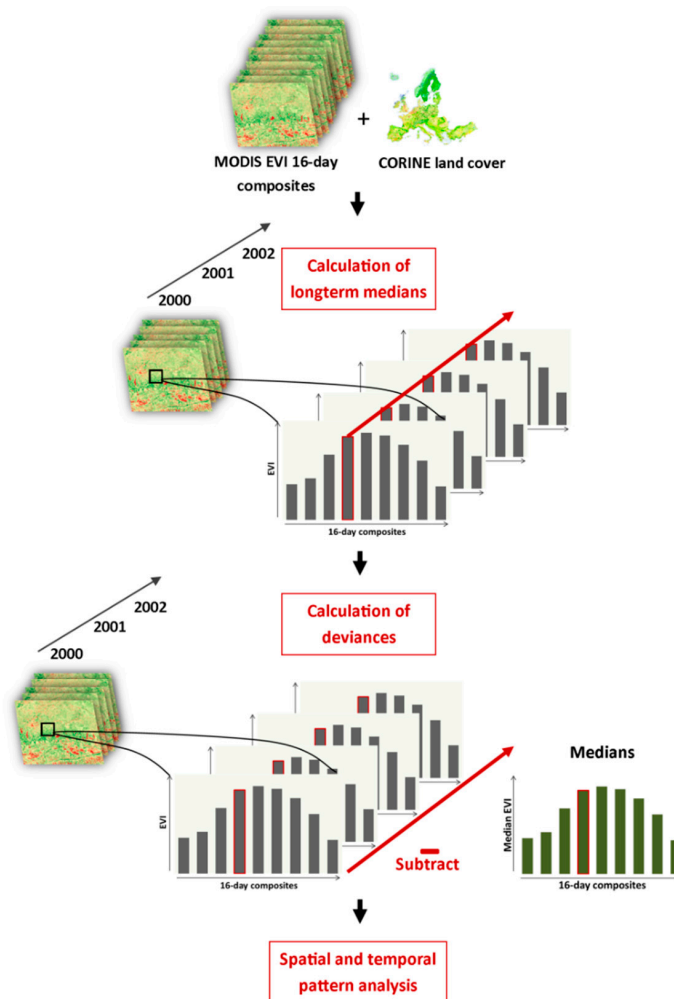


Figure 2. Schematic flowchart.

Table 1. Indication of the respective two 16-day composites used to create each monthly anomaly. For leap years, the start dates are one day earlier from March onward. The 23rd of April is used for the April composite and for the May composite.

Monthly Anomaly	Start Date of Composite 1	Start Date of Composite 2
Jan	1 January	17 January
Feb	2 February	18 February
Mar	6 March	22 March
Apr	7 April	23 April
May	23 April	9 May
Jun	25 May	10 June
Jul	26 June	12 July
Aug	28 July	13 August
Sep	29 August	14 September
Oct	30 September	16 October
Nov	1 November	17 November
Dec	3 December	19 December

In addition, deviations from the long-term median, which exceed two standard deviations (positive and negative), were analyzed. The number of MODIS pixels in Germany, for which the EVI value exceeds the pixel-based median plus and minus two standard deviations, respectively, were counted for each monthly composite. These pixel counts were calculated as percentages of the total amount of valid pixels to enable an investigation of the area in abnormal condition (positive and negative) within each month between 2000 and 2018.

Further, for analyzing the effect of droughts on specific land use/cover types, average EVI anomalies and the area with deviations exceeding two standard deviations were calculated for cropland, grassland, and forest. The investigated cropland consisted of irrigated and non-irrigated arable land and rice fields in accordance to the CORINE land cover classes 211, 212, and 213. Irrigated crops and rice are part of the included pre-defined crop types. However, they are almost completely absent in Germany, and effects of irrigation can be neglected. To analyze the drought within forests, broad-leaved, coniferous, and mixed forests, corresponding to the classes 311, 312, and 313, were combined. Grassland consisted of the classes 231 and 321, which are pastures and natural grasslands. Only MODIS pixels that were covered at least by 75% of the specific land cover type, according to the higher spatial resolution CLC 2012, were taken into account. When considering specific land cover types, it is possible that some counties include only small amounts of that land cover type, and displaying the county mean would not be representative. Thus, for the analysis of spatial patterns of EVI deviances in cropland and grassland, counties with a valid pixel count of less than 10 are excluded and shown as no data in the maps.

4. Results

4.1. Multi-Annual Temporal Patterns of Vegetation Anomalies

Figure 3 shows the seasonally averaged EVI deviances for Germany including all vegetated land cover types. The colors indicate the season's spring (green), summer (orange), and autumn (violet). Major negative anomalies are visible in 2003, 2006, 2010, 2013, and 2018, with most strong deviations occurring in spring whereas negative effects in the vegetation condition in summer and autumn are only present in 2003 and 2018. The year 2003 has permanent negative EVI anomalies throughout the entire growing season. The vegetation period of 2018 starts with a positive vegetation status compared to the long-term median, and only later in the year, vegetation condition are below average.

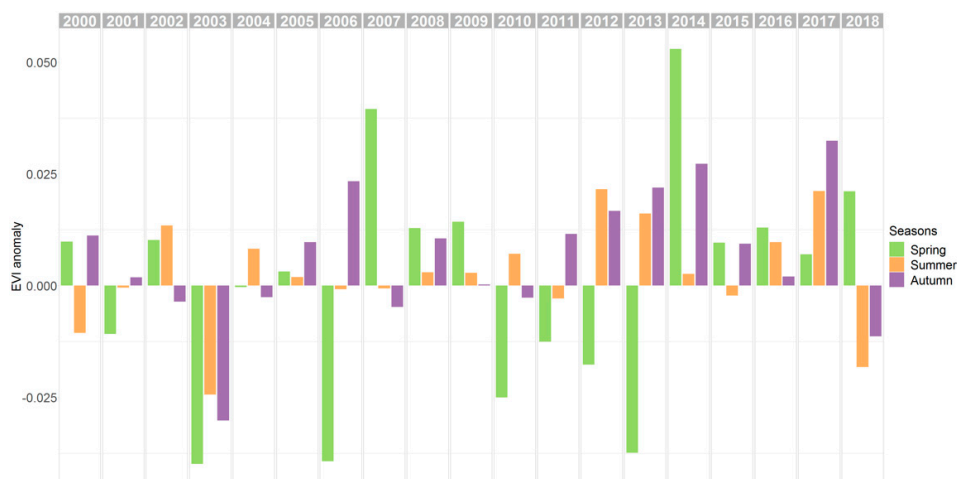


Figure 3. Seasonally averaged Enhanced Vegetation Index (EVI) anomalies for Germany for the years 2000–2018.

In Figure 4, monthly EVI deviances are shown in order to exhibit the temporal dynamics of the vegetation condition at finer temporal detail. In 2003 especially the spring and late summer months show negative effects (EVI deviances of -0.051 in March and -0.047 in August, percentage of deviances smaller two stdv of 7% in March and 9% in August), whereas June and October are close to average. The area of EVI variances per month exceeding two standard deviations reveals a relatively similar pattern compared to the monthly anomalies in 2003. There are strong negative anomalies in March and April 2006 and in April 2013; however, the areas of EVI deviances more negative than two standard deviations in these months are smaller compared to the affected areas in August and September of

2003 and 2018. In April and May 2018, a positive deviation compared to the other years and areas of around 14% with EVI deviations higher than two standard deviations are visible. From June onward, the negative anomaly becomes stronger during summer and autumn (EVI deviance of -0.039 and percentage of deviances smaller two stdv of 10% in September) until November, which shows a slightly positive effect in vegetation status. In particular, in June, the areas exceeding two standard deviations positively and negatively are almost identical, revealing heterogeneous conditions within the vegetated areas in Germany.

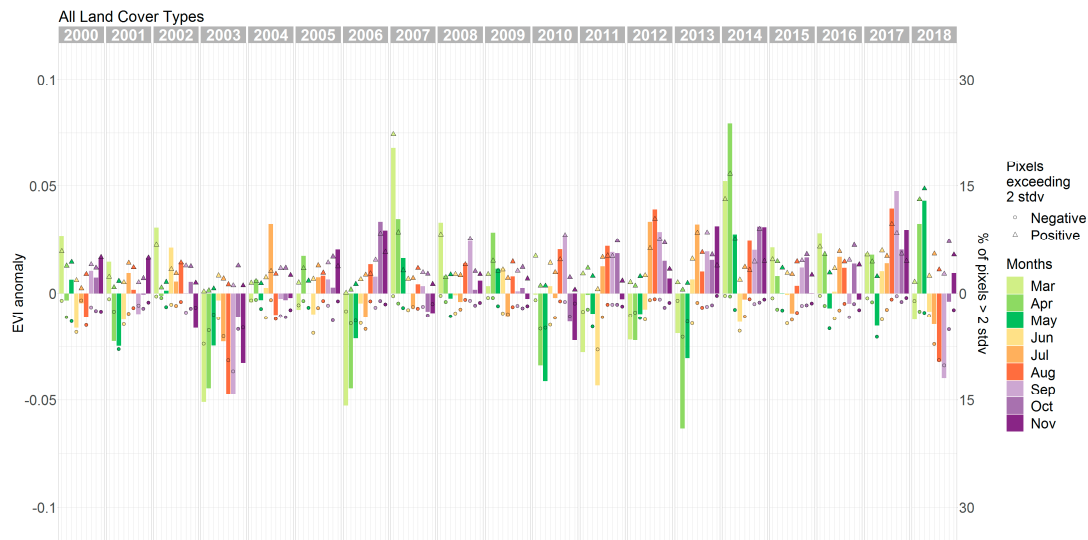


Figure 4. Monthly averaged EVI anomalies for all vegetated land cover types and percentage of pixels with EVI deviances exceeding two standard deviations (pixel-based) positively and negatively per month for Germany for the years 2000–2018 for all vegetated land cover types.

When only cropland is considered, the patterns are relatively similar (Figure 5), apart from April and May 2018, which show less positive effects than when averaging over all vegetated land cover types (Figure 4). In addition, the year 2011 reveals negative conditions for cropland, in particular in June, when combining the negative deviations from the long-term median and the amount of pixels, which are more negative than two standard deviations.

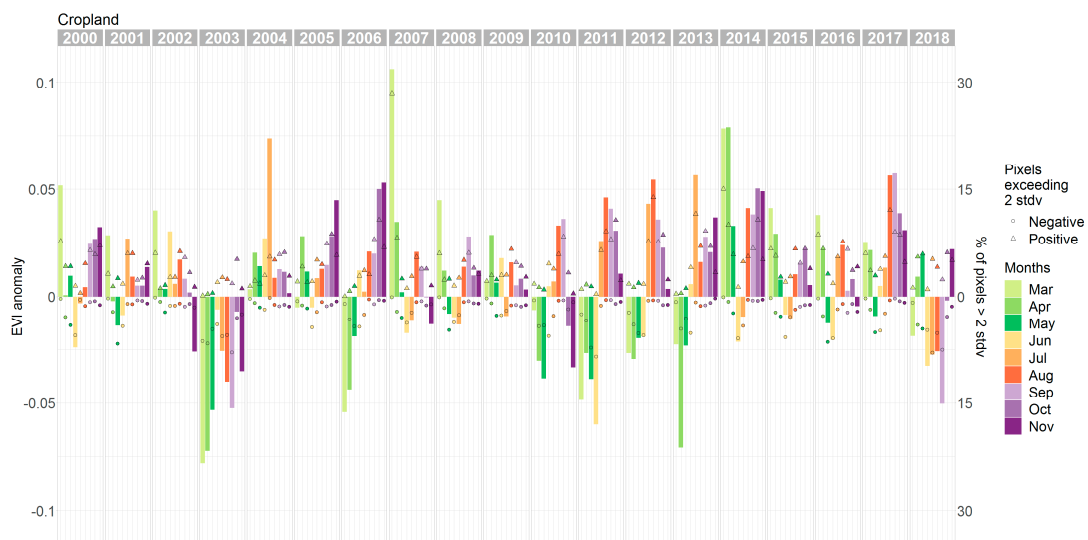


Figure 5. Monthly averaged EVI anomalies for cropland and percentage of pixels with EVI deviances exceeding two standard deviations (pixel-based) positively and negatively per month for Germany for the years 2000–2018 for cropland.

The pattern for grasslands (Figure 6) is also similar to the overall vegetation class patterns (Figure 4), revealing basically the same months being affected by anomalies. However, August and September 2003 as well as 2018 exhibit stronger negative grassland conditions than for the all vegetation class, which is also clearly visible in the percentage of area with EVI deviations smaller than two standard deviations (percentage of deviances smaller two stdv of 19% in August 2003 and 27% in August 2018). Considering only forested areas, however, leads to a different picture of EVI anomalies (Figure S1). There are minor negative effects visible in the spring months of 2006, 2010, and 2013. In general, the first years of the study period show negative anomalies, and the later years positive ones for forest areas, indicating a slight long-term tendency toward increasing EVI values.

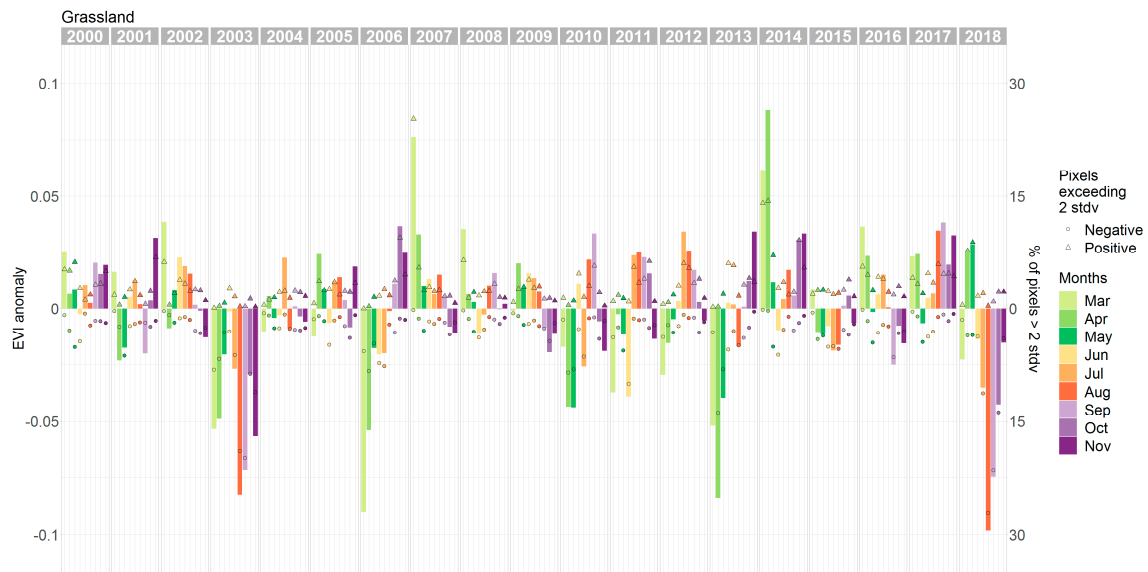


Figure 6. Monthly averaged EVI anomalies for grassland and percentage of pixels with EVI deviations exceeding two standard deviations (pixel-based) positively and negatively per month for Germany for the years 2000–2018 for grassland.

4.2. Spatial Patterns of Vegetation Anomalies

For the spatial investigation of vegetation status, the monthly EVI anomalies of 2003, 2004, 2006, and 2018 are shown as county means (Figure 7). These years have been chosen because 2003 and 2018 are both extraordinary in their negative effects in summer and autumn, as was seen in the temporal anomaly dynamics (Figures 3–6). The year 2006 shows more negative vegetation conditions in spring. The year 2004 is selected as an example of a year with average conditions because when adding up all absolute monthly EVI deviance values for each year, 2004 turns out to be the most average year of the selected 18 years period.

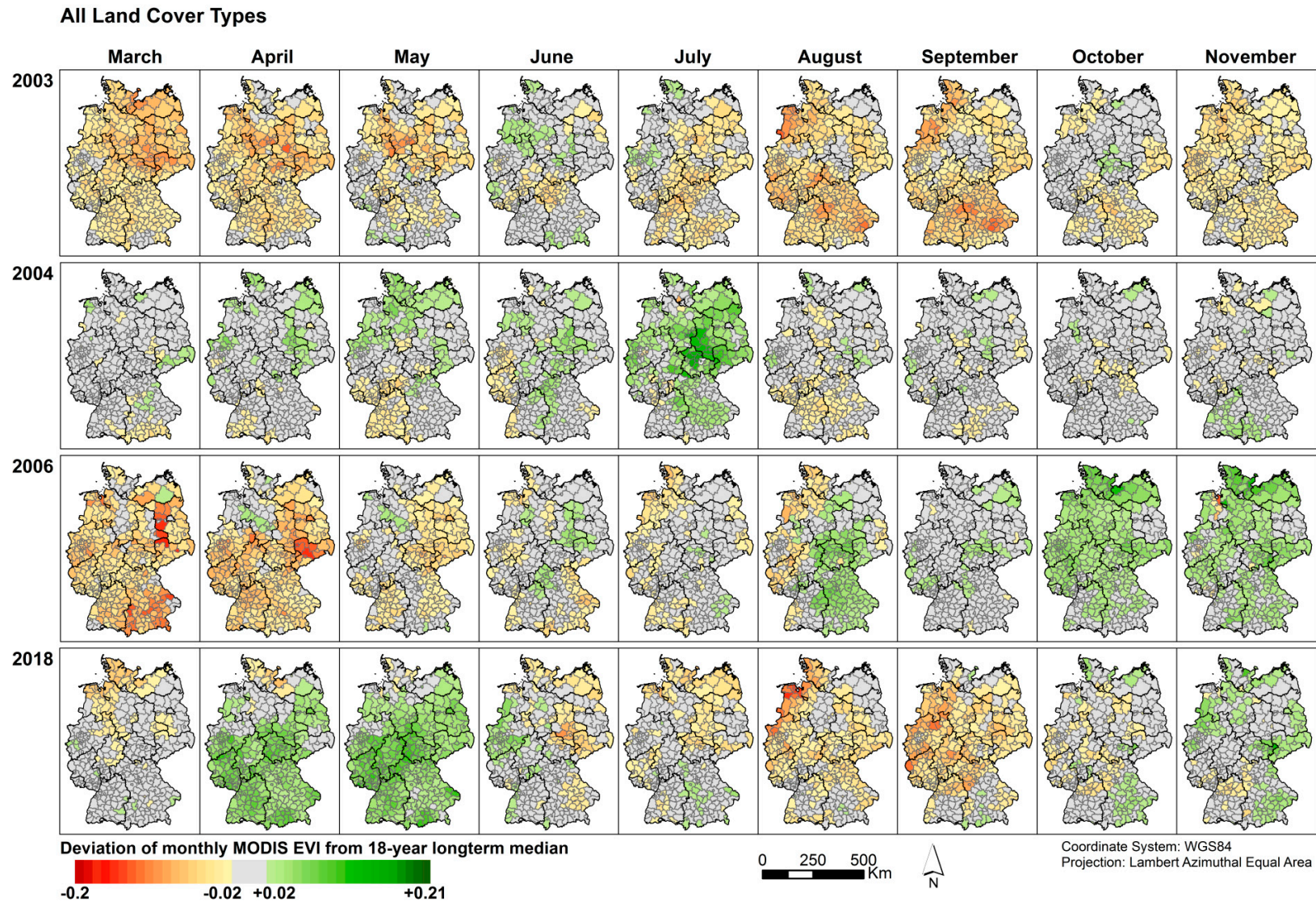


Figure 7. County level monthly EVI anomalies for the vegetation period of four years, including all vegetated land cover types.

Strong regional differences are visible, particularly considering negative EVI anomalies. In spring 2003, northeastern Germany reveals negative EVI anomalies, and during summer, negative effects are visible in southern and western parts (Figure 7). Almost no positive anomalies are detectable in the counties in 2003. The year 2004 shows almost no strong anomalies from the long-term median, apart from July, exhibiting relatively positive vegetation conditions in central Germany. In 2006, southern and northeastern areas show negative conditions for the vegetation compared to other years in March and April and improve in the course of the year with positive anomalies at the end of the vegetation period. April and May 2018 show positive effects in a large part of Germany. Negatively affected areas in Germany in 2018 are the most northern part at the beginning of the vegetation period, northeastern parts in June and July, and larger parts of Germany, especially in the northwestern region, in August and September. Overall the analysis of the intensity of the 2018 vegetation anomalies reveals highly variable local conditions even among neighboring counties.

Figure 8 shows EVI anomalies on county level for cropland for the same years as in Figure 7. The spatial anomaly patterns are basically similar; however, some areas show stronger negative conditions than for the overall vegetation class. In 2003, cropland areas in northeastern Germany seem highly affected at the beginning of the vegetation period and also southern parts in August and September show stronger negative anomalies. July 2004 shows a strong positive EVI deviance from the long-term mean in central Germany. In 2018, the negative vegetation status in the north in spring is enhanced and the positive effects in April and May less visible compared to the overall vegetation behavior. Negative anomalies in June 2018 are stronger.

The spatial analysis of grasslands for the same years shows stronger negative anomalies compared to cropland in August and September for both 2003 and 2018 (Figure S2). In both years, in particular in 2018, larger areas are also affected.

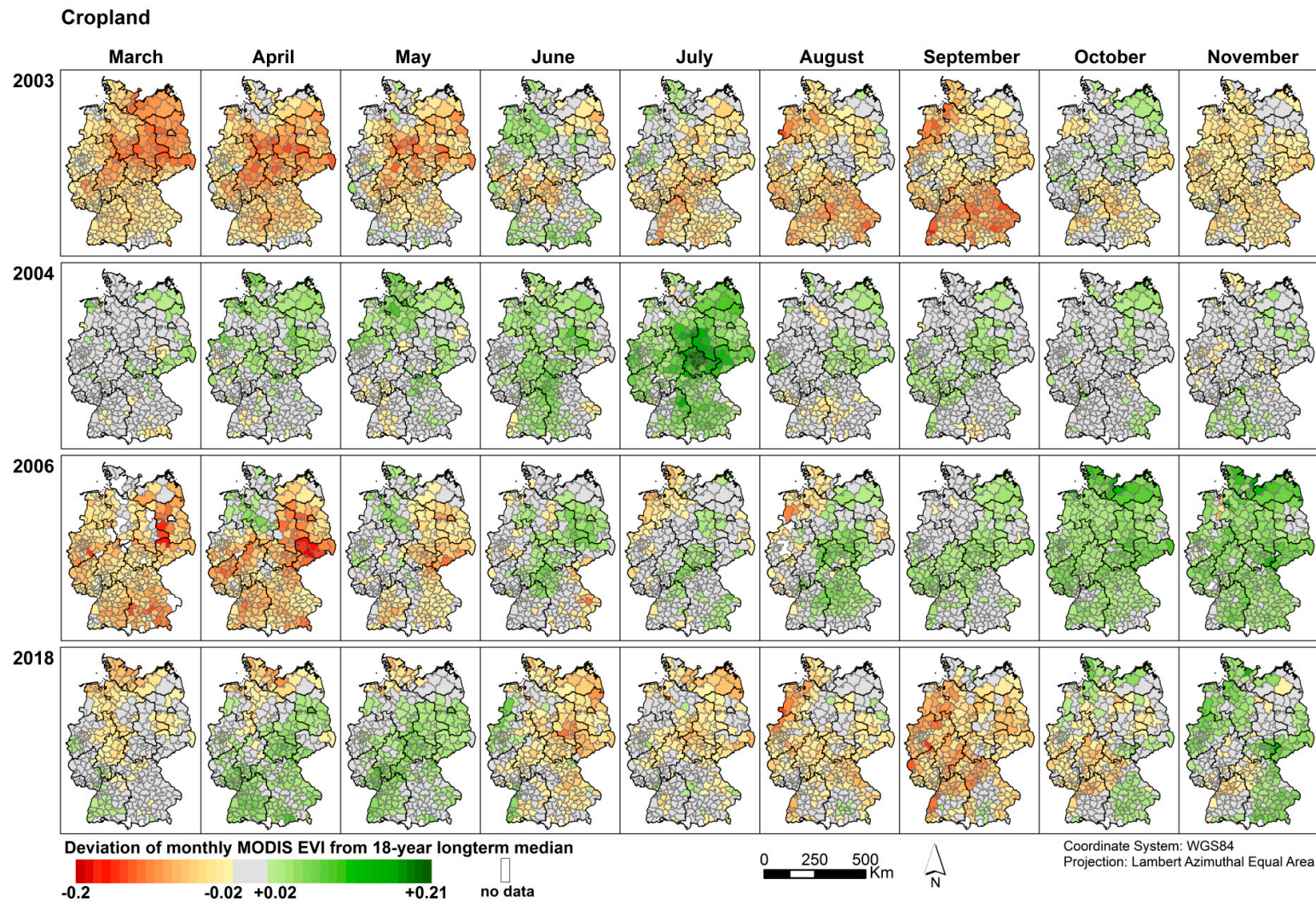


Figure 8. County level monthly EVI anomalies for the vegetation period of four years, including only croplands. Counties comprising less than 10 valid pixels are excluded and are shown as no data class.

4.3. Comparison with Yield Statistics

Annual yield statistics for different crop types were compared to the satellite-detected vegetation stress situations. The depicted crops (Figure 9) are winter wheat (A), rye and winter cereal (B), silage maize (C), and potatoes (D). The harvests are drawn as decitonne per hectare to prevent influence of changing cultivation quantities. Annual crop yields below one standard deviation from the mean are displayed in orange, which is the case for all four crops in 2003 and 2018. Apart from these two years, 2006, 2007, 2011, and 2013 reveal yields below one standard deviation from the mean for some of the crops.

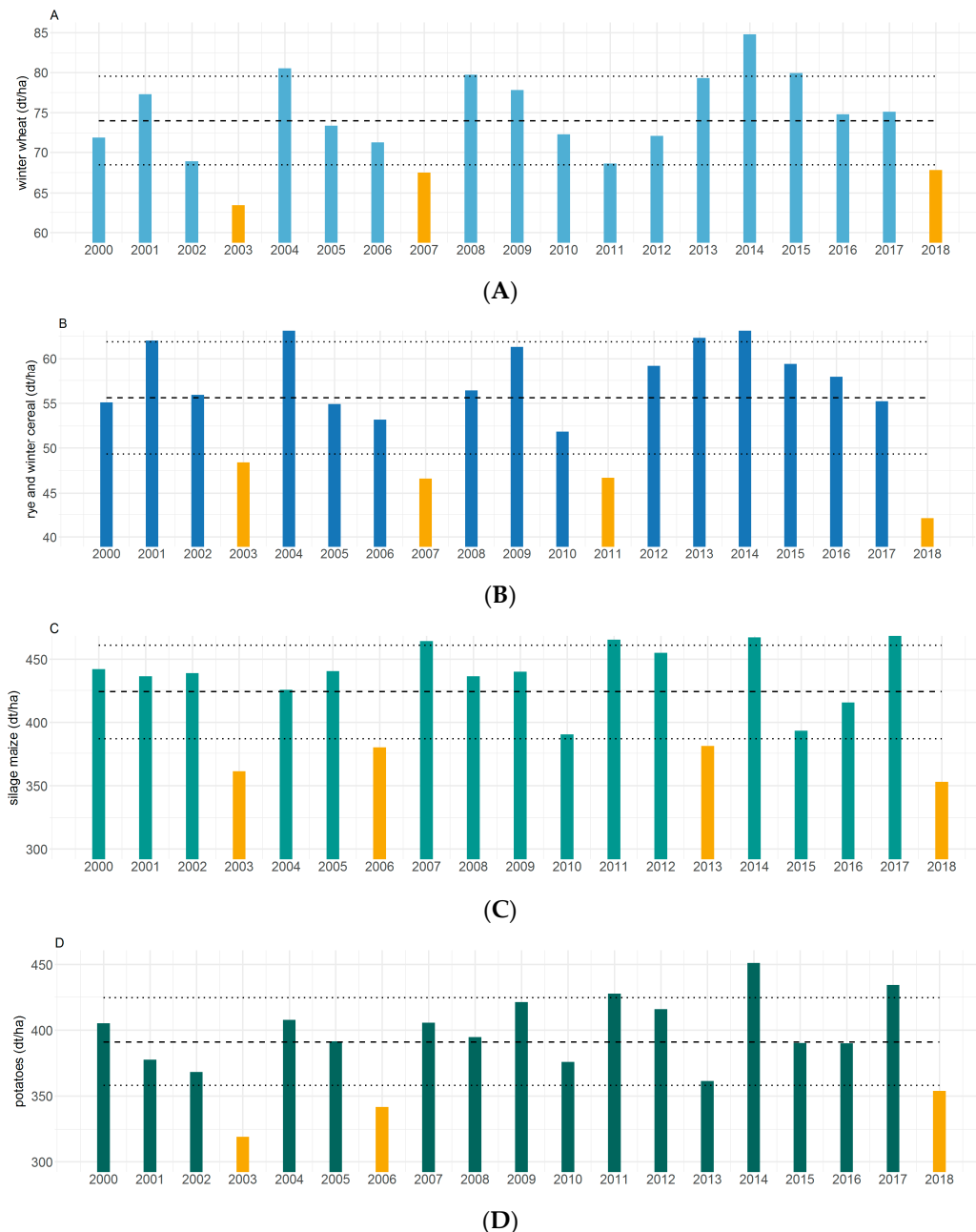


Figure 9. Yield statistics of Germany for the years 2000–2018 from the federal statistics office for four different crops [31]: winter wheat (A), rye and winter cereal (B), silage maize (C), and potatoes (D). The dashed line shows the mean yield and the dotted lines one standard deviation from the mean for the period of interest. Bars in orange are below the standard deviation. Be aware that the origin of the y-axis is non-zero in all four plots.

5. Discussion

5.1. The Most Extreme Years of the Study Period

The drought event of 2018 is clearly discernable from the used earth observation data and a high temporal and spatial variability could be revealed. The years 2003 and 2018 stand out as they are the only two years of the period of study showing strong negative anomalies in summer and autumn. Overall, we found that the negative vegetation condition anomaly of 2018 was not more extreme than in 2003, in particular because the beginning of the vegetation period 2018 showed positive deviations, while the year 2003 already showed negative deviations in spring. In addition, the spatial variation in vegetation condition was larger in 2018, which becomes visible when observing the areas with EVI values exceeding two standard deviations in a positive and a negative direction. These are the major differences between the drought years 2003 and 2018. It becomes clear that there is not a typical German or central European drought course or pattern, as characteristics differ, complicating early warning systems and counteracting management strategies at an early stage.

5.2. Comparison of EVI Anomalies with Weather Data and Crop Yields

5.2.1. The Years 2003 and 2018

Comparing the negative anomalies in vegetation condition to other data sets, such as meteorological data or yield statistics, supports the identified drought patterns. A recent study has shown that the dry and hot weather conditions of 2018 are connected to an amplified hemisphere-wide wavenumber 7 circulation pattern [35]. The same atmospheric circulation pattern was present during the European meteorological drought and/or heat events of 2003, 2006, and 2015 [35]. In 2018, patterns of precipitation deficit (Figure S3) and the spatial picture of EVI deviances are relatively similar with a lag of approximately one month. This is especially the case for May/June onwards. At the beginning of the vegetation period of 2018, the weather conditions were already dry and warm [36]. However, the spatial patterns were heterogeneous, with a dry north and strong precipitation events in the rest of Germany [36]. We revealed that the vegetation was overall not yet stressed under these conditions. Apart from small areas in the north, EVI deviances were actually positive in April and May 2018. This leads to the assumption that the plant-available water was not a limiting factor in spring and that the high temperatures were triggering an early phenological onset [36]. The water availability assumingly became too low only later in the year, as the vegetation photosynthetic activity was discernably below average. In contrast, the entire year 2003 was very dry in large parts of Germany and from May onward was extremely hot, especially in June and in August [37,38]. Apart from some areas in southeastern Germany, which experienced strong precipitation events in summer 2002, the year 2003 already started rather dry from a hydrological perspective as discharges were already lower than normal [39] and spring conditions were relatively dry [37]. Plant-available water was therefore limited, which is also visible in the negative vegetation conditions from the beginning of the vegetation period in 2003 revealed in this study. This is also supported by the analysis of the effects of high temperatures and water shortage on plant physiology and biochemistry, showing that heat only has a negative influence during dry conditions and not in moist conditions [28,40].

Regarding the crop yields of the considered field crops, both 2003 and 2018 were below one standard deviation from the mean for the different crop types. For two crops (potatoes and winter wheat), the harvests were lowest in 2003, for rye and winter cereal and silage maize in 2018. It can be assumed that, for the agricultural sector, the negative consequences of these two extreme years were similar, with differing effects on different crop types, depending on their water requirements at crucial phases throughout the year. The major difference was the positive start of 2018, especially the ripening phase of crops that was affected in this year, leading to large yield losses.

5.2.2. EVI Deviances and Their Drivers in Other Years

Apart from 2003 and 2018, we could depict the following years standing out with negative EVI anomalies or below-average yields: 2006, 2007, 2010, 2011, and 2013.

The year 2006 reached low yields in maize and potatoes and was characterized by varying weather conditions throughout the year. July 2006 reached the highest temperatures ever recorded at that time [41,42]. At the same time, in total, precipitation amounts were relatively normal, and in particular, a wet August prevented large damages due to the heatwave [41]. However, winter 2005/2006 lasted relatively long with cold temperatures until the second half of March [41]. This is in accordance with the EVI anomaly pattern of 2006 of this study, showing relatively negative conditions for the vegetation at the beginning of the vegetation period, but with below-average temperatures being the limiting factor at the time. Both the heatwave and the long-lasting winter might have reduced yields in 2006.

Crop statistics of 2007 show yields below-average for winter wheat and for rye and winter cereal. March and April 2007 were relatively warm and dry, May 2007 was very wet [43]. The EVI signal shows positive effects in March 2007, which are probably a result of the warm conditions in the phase of phenological onset. The vegetation stress level seems to be minimized through the wet May [43]. However, reduced harvests in cereal might have occurred as, due to the spring drought, a reduced number of ears were developed [44]. Such a small-scale effect is not visible in the EVI anomaly pattern. Another known drought year occurring majorly in Eastern Europe/Eurasia was 2010 [10], which is also visible within the time series showing negative vegetation condition.

The year 2011 shows strong negative values in particular in the EVI anomalies for cropland. The EVI deviances (Figure 5) reveal negative effects in the first half of the year with June being the most affected month, the second half is positive. The crop yield statistics also show below-average harvests, but only for rye and winter cereal. It can be assumed that these effects were caused by unfavorable cultivation conditions (wet and cold) in winter 2010/2011 [45], which lead to recorded damages of winter cereal. In addition to that, relatively dry conditions in western parts of Germany in spring (especially in May) had some negative influence on the cultivation of field crops [45].

We also found negative effects in EVI in April 2013. The reason for that are most probably also not dry or hot weather conditions, but a long-lasting winter and a late phenological onset as in large parts of Germany the snow cover was present until the second half of April [46]. This effect is also discernable in silage maize and—a little less prominently—in potato yields, but not in the winter cereals, highlighting the varying impacts of different abnormal weather conditions on different crop types.

Another notable year is 2015, as it was also dry and hot, especially in central and southern Germany [47]. However, within this study, no negative conditions for the vegetation were found considering the area of Germany. From a hydrological perspective, the drought was moderate and covered a smaller extent compared to 2003 [39]. Even if the meteorological situation was not so different from 2003 in some regions, water surplus from the preceding winter and spring 2015 prevented a hydrological drought [39]. This would explain the average EVI signal in 2015. This is also in accordance to the harvest statistics as none of the four investigated crops showed a yield below one standard deviation from the mean in 2015 at least averaged over Germany.

5.3. Effects for Different Land Cover Types

Within this study, we can depict variations in the characteristics of agricultural droughts for different land cover types. Croplands are managed, and management strategies are often adapted toward varying weather conditions. During drought conditions in summer, premature ripening potentially occurs in cereal, which has to be harvested earlier than normal. This was also the case for cereal crops in 2018, where major harvesting was already finished in mid of August [48]. In 2018, the situation in cropland relaxed in October and November. The more or less average EVI signal was possibly provoked by earlier than usual intermediate crop cultivations. The signal of intermediate crops is determined by a growing onset and greening of the intermediate crop vegetation and, therefore, leads to a normal EVI signal on average. In grassland, the vegetation stayed stressed until the very end

of the vegetation period. The negative EVI anomaly for grassland in Germany reached its maximum in August 2018 and stayed high. There was no recovery visible in parts until next year's spring (not shown). From an agricultural point of view, there was only one cut possible in agriculturally used grasslands in 2018, and no further harvesting was possible for the rest of the year [48]. Considering forests, no negative deviations could be observed in the drought year 2018 (Figure S1). We assume that the reaction of trees to drought has a larger lag or is not present at all, as trees are able to reach soil water from further below compared to crop or grass species [27,49]. In a study on the effects of the 2003 drought event on a central European deciduous forest [50], the trees did not show water stress, which would be in accordance with our findings. However, even though the EVI deviances are not strong, the year 2003 and the three following years (2004, 2005, and 2006) all show negative effects in our results. This might be a lagged effect of the 2003 drought. In another study, forests show a strongly delayed response to climate extreme conditions [27]. In 2018, especially April and May show positive effects in forested areas. In energy-limited regions higher temperatures and long sunshine durations can lead to higher photosynthetic activity of the vegetation. This might be especially true for forests, as trees reach deeper soil layers and have better access to soil water. A positive anomaly of photosynthetic activity during drought and heat conditions was also found in other studies for (central European) forests [27,49]. More research focused on drought effects on forests is needed to understand when negative (possibly long-term) impacts occur and when drought conditions trigger positive effects in forests.

There are several impacts of drought and heat events, such as a stress-related decrease in vegetation functioning or a complete destruction of the vegetation [9]. Water and chemical cycles and productivity of ecosystems are affected. Vegetation cover—in particular grasslands—react with increased evaporation to hot conditions, leading to an additional reduction of soil moisture and enhanced drought conditions [51]. This effect is assumed to have contributed to the extreme drought and heat in Europe in 2003 [51] and might also have played a role in 2018. It is expected to be a major influencing factor in future drought and heat events [52]. The effect on the carbon cycle is also of great importance as temperate ecosystems were assumed to increase carbon sequestration due to higher temperatures in future climates [53]. However, many ecosystem types possibly turn from carbon sink to carbon source, also in a long-term perspective [54,55], as the number of extreme events as heats and droughts will rise in the future [5]. The negative impact on productivity is especially problematic for the agricultural sector as yields and fodder are lost, which are often related to high additional costs. Drought and heat conditions influence yields negatively as physical and physiological damages and biochemical changes are induced, leading to reductions in plant growth and grain development, e.g., in cereal [56]. In addition, oil, starch, and protein content is negatively affected by high temperatures and water shortage in oilseed crops and cereals [56]. A typical reaction of plants to drought conditions is a shift in water use efficiency (WUE), which is defined as the ratio between dry matter and evapotranspiration [22,56]. In temperate regions, where vegetation shows poor adaption towards drought conditions [23], plants show an increase in WUE under dry conditions, which results in reduced biomass accumulation [56]. This is in accordance with a study analyzing the WUE with satellite-based GPP and evapotranspiration data, revealing a decreasing trend in WUE in the Northern Hemisphere [20]. An additional important drought characteristic influencing crop yields is the timing of water shortage. In a study from the Iberian Peninsula, it was found that cereal yield is especially reduced with limited soil moisture in early spring and high temperatures during harvesting time [57].

5.4. Suitability of the Methods Used

The MODIS 250 m remote sensing data seems to be sufficiently resolved to reveal drought patterns for different land cover types in the relatively heterogeneous landscapes of Germany, which are typical for central Europe. To date, the MODIS time series is one of the few satellite data sets allowing an assessment of vegetation condition in the long-term perspective of almost two decades with the necessary spatial and daily resolution crucial to detect highly variable phenological processes. Even the

promising, higher spatial resolution Copernicus data will not allow this kind of temporal classification for some time to come. The CORINE land cover map offers sufficient spatial resolution (100 m) to differentiate between different land cover types. Focusing on the status of the vegetation enables an assessment of agricultural droughts, which are strongly connected to socio-economic factors such as agricultural yields. The usage of satellite earth observation data allows an extensive investigation without the need of interpolation or modelling. A limitation of the study approach is the difficulty in disentangling drought effects, effects from other abnormal weather conditions such as snow water availability or frosts, and management strategies. As within this study, particularly unfavorable weather conditions in spring, like snow and frosts, were easily confused with drought or heat events, so including snow cover information [58] would support a more comprehensive detection of the effects of dry and hot weather. In addition, there might be uncertainties introduced through crop rotation. An investigation on the level of different crop types might be an interesting next step, making a detailed crop type classification with high spatial resolution necessary [59]. Another important aspect is irrigation, as irrigated croplands or grasslands can distort the effects of drought on vegetation. In Germany, only 2.5% [31] of agricultural area was irrigated in 2018, so the effect can be considered as minimal. In addition, it has to be kept in mind that the approach constitutes an analysis of extreme conditions within the study period only. It is not possible to make a statement about the magnitude of the detected extreme conditions compared to the years before 2000. Regarding the crop yield data, an uncertainty is potentially introduced as the crops, considering their drought resistance, might have changed during the last 20 years. More information on the cultivation of specific crop types is needed to take this into account.

6. Conclusions

The year 2018 was noticeably hot and dry, and such years are expected to become more frequent in Europe. Within this study, the vegetation condition of spring to autumn 2018 was investigated and compared to the growing period of the years 2000 to 2017.

When assessing the years with stressed vegetation and yield losses between 2000 and 2018 more closely, it becomes clear that 2003 and 2018 are extraordinary as they are the only years showing strong negative effects in summer and autumn due to drought conditions. However, the spatial pattern and temporal development between these drought years differ. The year 2018 had, in terms of annual crop yields, a similar effect as 2003, even though the year started favorably, with vegetation conditions in April and May more positive compared to other years. The spatial and temporal variability was higher in 2018 than in 2003, highlighting the heterogeneity of vegetation condition in Germany in 2018. Within the study we also revealed the differing effects of drought conditions on various land cover types. Within croplands, the year 2011 showed stronger negative conditions—next to 2003 and 2018—when compared to other land cover types. Overall, grassland exhibits the strongest EVI deviances during drought conditions. In addition, patterns of reduced vegetation vigor within other years could be depicted on a monthly scale, e.g., 2006, 2010, 2011, and 2013. These years were partly characterized by dry and hot conditions. However, long-lasting winters with late phenological onsets and frosts were also often the reason for negative vegetation development. When these dynamics occur in spring months, additional information on weather conditions is important to understand the influencing factors.

Including snow cover data would improve the comprehension of reduced EVI signals in spring. Adding soil moisture information might support the interpretation of diverging effects of weather and vegetation condition. Furthermore, a crop-specific analysis would be interesting in the future, as yield losses varied between crop types and the effects of the timing of the drought and heat event might become clearer.

Supplementary Materials: The following are available online at <http://www.mdpi.com/2072-4292/11/15/1783/s1>, Figure S1: Monthly averaged EVI anomalies and percentage of pixels, which are more negative than the median minus two standard deviations and pixels, which are more positive than the median plus two standard deviations

for Germany for the years 2000–2018 for forest, Figure S2: County-level monthly EVI anomalies for the vegetation period of four years, including only grasslands. Counties comprising less than 10 valid pixels are excluded and are shown as no data class, Figure S3: Monthly Standardized Precipitation Index (one month) of Germany for 2018 provided by DWD (Deutscher Wetterdienst).

Author Contributions: S.D. had the idea for the research question; U.G., S.A., and S.R. designed the study; S.R. processed and analyzed the data; U.G., S.A., C.K., and S.R. discussed the results together; S.A. and U.G. helped in visualization; S.R. wrote the original draft; U.G. and S.A. helped writing; U.G., S.A., and C.K. reviewed the draft.

Funding: This research received no external funding.

Acknowledgments: We gratefully acknowledge the anonymous reviewers for constructive comments for improvement of the manuscript. We would like to thank the DWD (Deutscher Wetterdienst) for the provided Standardized Precipitation Index data of the year 2018.

Conflicts of Interest: The authors declare no conflict of interest.

References

- Masante, D.; Vogt, J. Drought in Central-Northern Europe—August 2018. 2018. Available online: http://edo.jrc.ec.europa.eu/documents/news/EDODroughtNews201808_Central_North_Europe.pdf (accessed on 14 June 2019).
- IPCC. *Global Warming of 1.5 °C; An IPCC Special Report on the Impacts of Global Warming of 1.5 °C above Pre-Industrial Levels and Related Global Greenhouse Gas Emission Pathways, in the Context of Strengthening the Global Response to the Threat of Climate Change, Sustainable Development, and Efforts to Eradicate Poverty*; 2018. Available online: <https://www.ipcc.ch/sr15/> (accessed on 26 July 2019).
- IPCC. *Climate Change 2013: The Physical Science Basis; Contribution of Working Group I to the Fifth Assessment Report of the Intergovernmental Panel on Climate Change*; 2013. Available online: <https://www.ipcc.ch/report/ar5/wg1/> (accessed on 26 July 2019).
- Suarez-Gutierrez, L.; Li, C.; Müller, W.A.; Marotzke, J. Internal variability in European summer temperatures at 1.5 °C and 2 °C of global warming. *Environ. Res. Lett.* **2018**, *13*, 064026. [[CrossRef](#)]
- Spinoni, J.; Vogt, J.V.; Naumann, G.; Barbosa, P.; Dosio, A. Will drought events become more frequent and severe in Europe? *Int. J. Climatol.* **2018**, *38*, 1718–1736. [[CrossRef](#)]
- Samaniego, L.; Thober, S.; Kumar, R.; Wanders, N.; Rakovec, O.; Pan, M.; Zink, M.; Sheffield, J.; Wood, E.F.; Marx, A. Anthropogenic warming exacerbates European soil moisture droughts. *Nat. Clim. Chang.* **2018**, *8*, 421. [[CrossRef](#)]
- Grillakis, M.G. Increase in severe and extreme soil moisture droughts for Europe under climate change. *Sci. Total Environ.* **2019**, *660*, 1245–1255. [[CrossRef](#)] [[PubMed](#)]
- De Bono, A.; Guiliani, G.; Kluser, S.; Peduzzi, P. Impacts of Summer 2003 Heat Wave in Europe. 2018. Available online: https://www.unisdr.org/files/1145_ewheatwave.en.pdf (accessed on 14 June 2019).
- Crausbay, S.D.; Ramirez, A.R.; Carter, S.L.; Cross, M.S.; Hall, K.R.; Bathke, D.J.; Betancourt, J.L.; Colt, S.; Cravens, A.E.; Dalton, M.S.; et al. Defining Ecological Drought for the Twenty-First Century. *Bull. Am. Meteorol. Soc.* **2017**, *98*, 2543–2550. [[CrossRef](#)]
- Bastos, A.; Gouveia, C.M.; Trigo, R.M.; Running, S.W. Analysing the spatio-temporal impacts of the 2003 and 2010 extreme heatwaves on plant productivity in Europe. *Biogeosciences* **2014**, *11*, 3421–3435. [[CrossRef](#)]
- Gammans, M.; Mérel, P.; Ortiz-Bobea, A. Negative impacts of climate change on cereal yields: Statistical evidence from France. *Environ. Res. Lett.* **2017**, *12*, 054007. [[CrossRef](#)]
- Obermeier, W.A.; Lehnert, L.W.; Ivanov, M.A.; Luterbacher, J.; Bendix, J. Reduced Summer Aboveground Productivity in Temperate C3 Grasslands under Future Climate Regimes. *Earth's Future* **2018**, *6*, 716–729. [[CrossRef](#)]
- Imbery, F.; Friedrich, K.; Koppe, C.; Janssen, W.; Pfeifroth, U.; Daßler, J.; Bissolli, P. 2018 wärmster Sommer im Norden und Osten Deutschlands. 2018. Available online: https://www.dwd.de/DE/leistungen/besondereereignisse/temperatur/20180906_waermstersommer_nordenosten2018.html (accessed on 14 December 2018).
- Hänsel, S.; Ustrnul, Z.; Lupikasza, E.; Skalak, P. Assessing seasonal drought variations and trends over Central Europe. *Adv. Water Resour.* **2019**, *127*, 53–75. [[CrossRef](#)]

15. BMEL. Vereinbarung für das Dürrehilfsprogramm Ist Jetzt von allen Teilnehmenden Bundesländern Unterzeichnet. 2018. Available online: https://www.bmel.de/SharedDocs/Pressemitteilungen/2018/155-Vereinbarung_Duerrehilfsprogramm.html (accessed on 14 June 2019).
16. Vicente-Serrano, S.M. Evaluating the Impact of Drought Using Remote Sensing in a Mediterranean, Semi-arid Region. *Nat. Hazards* **2007**, *40*, 173–208. [[CrossRef](#)]
17. Winkler, K.; Gessner, U.; Hochschild, V. Identifying Droughts Affecting Agriculture in Africa Based on Remote Sensing Time Series between 2000–2016: Rainfall Anomalies and Vegetation Condition in the Context of ENSO. *Remote Sens.* **2017**, *9*, 831. [[CrossRef](#)]
18. Gouveia, C.M.; Trigo, R.M.; Beguería, S.; Vicente-Serrano, S.M. Drought impacts on vegetation activity in the Mediterranean region: An assessment using remote sensing data and multi-scale drought indicators. *Glob. Planet. Chang.* **2017**, *151*, 15–27. [[CrossRef](#)]
19. Zscheischler, J.; Mahecha, M.D.; Harmeling, S.; Reichstein, M. Detection and attribution of large spatiotemporal extreme events in Earth observation data. *Ecol. Inform.* **2013**, *15*, 66–73. [[CrossRef](#)]
20. Yu, Z.; Wang, J.; Liu, S.; Rentch, J.S.; Sun, P.; Lu, C. Global gross primary productivity and water use efficiency changes under drought stress. *Environ. Res. Lett.* **2017**, *12*, 014016. [[CrossRef](#)]
21. Vicente-Serrano, S.M.; Gouveia, C.; Camarero, J.J.; Beguería, S.; Trigo, R.; López-Moreno, J.I.; Azorín-Molina, C.; Pasho, E.; Lorenzo-Lacruz, J.; Revuelto, J.; et al. Response of vegetation to drought time-scales across global land biomes. *Proc. Natl. Acad. Sci. USA* **2013**, *110*, 52–57. [[CrossRef](#)] [[PubMed](#)]
22. Ahmadi, B.; Ahmadi, A.; Tootle, G.; Moradkhani, H. Remote sensing of water use efficiency and terrestrial drought recovery across the contiguous united states. *Remote Sens.* **2019**, *11*, 731. [[CrossRef](#)]
23. Ivits, E.; Horion, S.; Fensholt, R.; Cherlet, M. Drought footprint on European ecosystems between 1999 and 2010 assessed by remotely sensed vegetation phenology and productivity. *Glob. Chang. Biol.* **2014**, *20*, 581–593. [[CrossRef](#)] [[PubMed](#)]
24. Le Page, M.; Zribi, M. Analysis and predictability of drought in Northwest Africa using optical and microwave satellite remote sensing products. *Sci. Rep.* **2019**, *9*, 1466. [[CrossRef](#)] [[PubMed](#)]
25. Reichstein, M.; Ciais, P.; Papale, D.; Valentini, R.; Running, S.; Viovy, N.; Cramer, W.; Granier, A.; Ogee, J.; Allard, V.; et al. Reduction of ecosystem productivity and respiration during the European summer 2003 climate anomaly: A joint flux tower, remote sensing and modelling analysis. *Glob. Chang. Biol.* **2007**, *13*, 634–651. [[CrossRef](#)]
26. Vicca, S.; Balzarolo, M.; Filella, I.; Granier, A.; Herbst, M.; Knohl, A.; Longdoz, B.; Mund, M.; Nagy, Z.; Pintér, K.; et al. Remotely-sensed detection of effects of extreme droughts on gross primary production. *Sci. Rep.* **2016**, *6*, 28269. [[CrossRef](#)] [[PubMed](#)]
27. Nicolai-Shaw, N.; Zscheischler, J.; Hirschi, M.; Gudmundsson, L.; Seneviratne, S.I. A drought event composite analysis using satellite remote-sensing based soil moisture. *Remote Sens. Environ.* **2017**, *203*, 216–225. [[CrossRef](#)]
28. Zandalinas, S.I.; Mittler, R.; Balfagón, D.; Arbona, V.; Gómez-Cadenas, A. Plant adaptations to the combination of drought and high temperatures. *Physiol. Plant.* **2018**, *162*, 2–12. [[CrossRef](#)] [[PubMed](#)]
29. Reichstein, M.; Bahn, M.; Ciais, P.; Frank, D.; Mahecha, M.D.; Seneviratne, S.I.; Zscheischler, J.; Beer, C.; Buchmann, N.; Frank, D.C.; et al. Climate extremes and the carbon cycle. *Nature* **2013**, *500*, 287. [[CrossRef](#)] [[PubMed](#)]
30. DWD. Monthly Temperature and Precipitation Data for the States of Germany. 2018. Available online: ftp://ftp-cdc.dwd.de/pub/CDC/regional_averages_DE/monthly/ (accessed on 1 February 2019).
31. Destatis. Genesis-Online: Datenlizenz by-2-0. Available online: <https://www-genesis.destatis.de/genesis/online/logon> (accessed on 14 June 2019).
32. EEA. CORINE Land Monitoring Service 2012. 2012. Available online: <https://land.copernicus.eu/pan-european/corine-land-cover> (accessed on 9 November 2018).
33. Didan, K. MOD13Q1 MODIS/Terra Vegetation Indices 16-Day L3 Global 250m SIN Grid V006 [Data set]. NASA EOSDIS Land Processes DAAC. 2015. Available online: <https://lpdaac.usgs.gov/products/mod13q1v006/> (accessed on 29 July 2019).
34. Gorelick, N.; Hancher, M.; Dixon, M.; Ilyushchenko, S.; Thau, D.; Moore, R. Google Earth Engine: Planetary-scale geospatial analysis for everyone. *Remote Sens. Environ.* **2017**, *202*, 18–27. [[CrossRef](#)]

35. Kornhuber, K.; Osprey, S.; Coumou, D.; Petri, S.; Petoukhov, V.; Rahmstorf, S.; Gray, L. Extreme weather events in early summer 2018 connected by a recurrent hemispheric wave-7 pattern. *Environ. Res. Lett.* **2019**, *14*, 054002. [[CrossRef](#)]
36. Imbery, F.; Friedrich, K.; Fleckenstein, R.; Kaspar, F.; Ziese, M.; Fildebrandt, J.; Schube, C. Mai 2018: Zweiter Monatlicher Temperaturrekord in Folge, Regional mit Dürren und Starkniederschlägen. 2018. Available online: https://www.dwd.de/DE/leistungen/besondereereignisse/temperatur/20180604_bericht_mai2018.pdf (accessed on 17 June 2019).
37. Müller-Westermeier, G.; Riecke, W. Die Witterung in Deutschland. In *Klimastatusbericht 2003*; DWD, Ed.; DWD (Deutscher Wetterdienst): Offenbach, Germany, 2004; pp. 71–78.
38. Rebetez, M.; Mayer, H.; Dupont, O.; Schindler, D.; Gartner, K.; Kropp, J.P.; Menzel, A. Heat and drought 2003 in Europe: A climate synthesis. *Ann. For. Sci.* **2006**, *63*, 569–577. [[CrossRef](#)]
39. Laaha, G.; Gauster, T.; Tallaksen, L.M.; Vidal, J.-P.; Stahl, K.; Prudhomme, C.; Heudorfer, B.; Vlnas, R.; Ionita, M.; van Lanen, H.A.J.; et al. The European 2015 drought from a hydrological perspective. *Hydrol. Earth Syst. Sci.* **2017**, *21*, 3001–3024. [[CrossRef](#)]
40. Matiu, M.; Ankerst, D.P.; Menzel, A. Interactions between temperature and drought in global and regional crop yield variability during 1961–2014. *PLoS ONE* **2017**, *12*, 1–23. [[CrossRef](#)]
41. Müller-Westermeier, G.; Lefebvre, C.; Nitsche, H.; Riecke, W.; Zimmermann, K. Die Witterung in Deutschland 2006. In *Klimastatusbericht 2006*; DWD, Ed.; DWD (Deutscher Wetterdienst): Offenbach, Germany, 2007; pp. 5–27.
42. Rebetez, M.; Dupont, O.; Giroud, M. An analysis of the July 2006 heatwave extent in Europe compared to the record year of 2003. *Theor. Appl. Climatol.* **2009**, *95*, 1–7. [[CrossRef](#)]
43. Müller-Westermeier, G.; Lefebvre, C.; Nitsche, H.; Riecke, W.; Zimmermann, K. Die Witterung in Deutschland. In *Klimastatusbericht 2007*; DWD, Ed.; DWD (Deutscher Wetterdienst): Offenbach, Germany, 2008; pp. 25–49.
44. Löpmeier, F.-J.; Trampf, W. Die agrarmeteorologische Situation im Jahr 2007. In *Klimastatusbericht 2007*; DWD, Ed.; DWD (Deutscher Wetterdienst): Offenbach, Germany, 2008; pp. 50–60.
45. BMEL. Ernte 2011: Mengen und Preise. 2011. Available online: http://www.bmel-statistik.de/fileadmin/user_upload/monatsberichte/EQB-6011010-2011.pdf (accessed on 8 March 2019).
46. BMEL. Ernte 2013: Mengen und Preise. 2013. Available online: https://www.bmel.de/SharedDocs/Downloads/Landwirtschaft/Markt-Statistik/Ernte2013_Bericht+Anlagen.pdf (accessed on 8 March 2019).
47. Ionita, M.; Tallaksen, L.M.; Kingston, D.G.; Stagge, J.H.; Laaha, G.; van Lanen, H.A.J.; Scholz, P.; Chelcea, S.M.; Haslinger, K. The European 2015 drought from a climatological perspective. *Hydrol. Earth Syst. Sci.* **2017**, *21*, 1397–1419. [[CrossRef](#)]
48. BMEL. Ernte 2018: Mengen und Preise. 2018. Available online: <https://www.bmel.de/SharedDocs/Downloads/Landwirtschaft/Markt-Statistik/Ernte2018Bericht.pdf> (accessed on 7 March 2019).
49. Zscheischler, J.; Orth, R.; Seneviratne, S.I. A submonthly database for detecting changes in vegetation-atmosphere coupling. *Geophys. Res. Lett.* **2015**, *42*, 9816–9824. [[CrossRef](#)]
50. Leuzinger, S.; Zotz, G.; Asshoff, R.; Körner, C. Responses of deciduous forest trees to severe drought in Central Europe. *Tree Physiol.* **2005**, *25*, 641–650. [[CrossRef](#)] [[PubMed](#)]
51. Teuling, A.J.; Seneviratne, S.I.; Stöckli, R.; Reichstein, M.; Moors, E.; Ciais, P.; Luyssaert, S.; van den Hurk, B.; Ammann, C.; Bernhofer, C.; et al. Contrasting response of European forest and grassland energy exchange to heatwaves. *Nat. Geosci.* **2010**, *3*, 722–727. [[CrossRef](#)]
52. Seneviratne, S.I.; Lüthi, D.; Litschi, M.; Schär, C. Land-atmosphere coupling and climate change in Europe. *Nature* **2006**, *443*, 205–209. [[CrossRef](#)] [[PubMed](#)]
53. Cox, P.M.; Betts, R.A.; Jones, C.D.; Spall, S.A.; Totterdell, I.J. Acceleration of global warming due to carbon-cycle feedbacks in a coupled climate model. *Nature* **2000**, *408*, 184–187. [[CrossRef](#)] [[PubMed](#)]
54. Hoover, D.L.; Rogers, B.M. Not all droughts are created equal: The impacts of interannual drought pattern and magnitude on grassland carbon cycling. *Glob. Chang. Biol.* **2016**, *22*, 1809–1820. [[CrossRef](#)] [[PubMed](#)]
55. Ciais, P.; Reichstein, M.; Viovy, N.; Granier, A.; Ogée, J.; Allard, V.; Aubinet, M.; Buchmann, N.; Bernhofer, C.; Carrara, A.; et al. Europe-wide reduction in primary productivity caused by the heat and drought in 2003. *Nature* **2005**, *437*, 529–533. [[CrossRef](#)] [[PubMed](#)]
56. Fahad, S.; Bajwa, A.A.; Nazir, U.; Anjum, S.A.; Farooq, A.; Zohaib, A.; Sadia, S.; Nasim, W.; Adkins, S.; Saud, S.; et al. Crop Production under Drought and Heat Stress: Plant Responses and Management Options. *Front. Plant Sci.* **2017**, *8*, 1147. [[CrossRef](#)]

57. Ribeiro, A.F.S.; Russo, A.; Gouveia, C.M.; Páscoa, P. Modelling drought-related yield losses in Iberia using remote sensing and multiscalar indices. *Theor. Appl. Climatol.* **2019**, *136*, 203–220. [[CrossRef](#)]
58. Dietz, A.J.; Kuenzer, C.; Dech, S. Global SnowPack: A new set of snow cover parameters for studying status and dynamics of the planetary snow cover extent. *Remote Sens. Lett.* **2015**, *6*, 844–853. [[CrossRef](#)]
59. Orynbaikyzy, A.; Gessner, U.; Conrad, C. Crop type classification using a combination of optical and radar remote sensing data: A review. *Int. J. Remote Sens.* **2019**, *40*, 6553–6595. [[CrossRef](#)]



© 2019 by the authors. Licensee MDPI, Basel, Switzerland. This article is an open access article distributed under the terms and conditions of the Creative Commons Attribution (CC BY) license (<http://creativecommons.org/licenses/by/4.0/>).